

Highly microporous monodisperse silica spheres synthesized by the Stöber process



Piotr A. Bazuła¹, Pablo M. Arnal³, Carolina Galeano², Bodo Zibrowius, Wolfgang Schmidt*, Ferdi Schüth*

Max-Planck-Institut für Kohlenforschung, Kaiser-Wilhelm-Platz 1, D-45470 Mülheim an der Ruhr, Germany

ARTICLE INFO

Article history:

Received 4 March 2014

Revised 11 July 2014

Accepted 27 July 2014

Available online 9 August 2014

This paper is dedicated to Prof. Thomas Bein on the occasion of his 60th Birthday.

Keywords:

Silica

Spheres

High specific surface area

Thermal stability

ABSTRACT

Silica spheres that are prepared by the Stöber process are usually considered non-porous. Here we report on a slightly modified synthesis protocol that allows preparation of microporous Stöber particles. Successive treatment with water and alcohol at room temperature results in substantial reorganization of the silica within the Stöber particles. Hydrolysis of alkoxy groups as well as condensation and re-esterification of silanol groups upon re-immersion in alcohol are crucial for that process. As the result of the silica reorganization, micropore channels are formed within the particles. After a final washing with water to remove all alkoxy groups from the particles, pure microporous silica spheres are obtained. The total pore volumes of these materials are comparable to those of zeolitic materials.

© 2014 Elsevier Inc. All rights reserved.

1. Introduction

Monodisperse spherical silica particles that are synthesized with controlled particles size via the Stöber process [1] are used in various fields in industry and science, such as catalysis, chromatography, photonic crystals, colloids, or as templates for core-shell materials [2–10]. The monodisperse spherical silica particles are typically prepared from tetraethyl orthosilicate (TEOS) under basic conditions. The Stöber process itself is well established and most aspects of the method are understood. Reports can be found on particle nucleation and growth processes [11–23], microstructure of the particles [11,23], and surface modifications with polymers [24–28], alkyl amine [29–31], or silane coupling agents [32–37]. Stöber silica spheres are usually considered to be non-porous. However, the fact that gold particles that had been embedded in such silica spheres can be leached out indicates a certain porosity of the Stöber-type spheres [38]. The presence of pores in these silica particles could be due to specific synthesis protocols in the preparation of the embedded gold particles. Evidence for small

fractions of micropores within Stöber particles has been reported also by other authors [13,14,33,39]. Furthermore, the concentration of hydroxyl groups within such particles substantially exceeded the number of hydroxyl groups that could be accommodated on the particles' external surfaces, indicating a substantial amount of non-condensed silica within the particles [17,18,38,40]. Thus, porosity of Stöber-type particles seems to depend strongly on specific synthesis parameters.

During the synthesis of core-shell particles consisting of zirconia (or titania) shells on silica cores [10,41–43], we observed unexpectedly high specific surface areas of about $500 \text{ m}^2 \text{ g}^{-1}$ for $\text{SiO}_2@ZrO_2$ particles that had been obtained as intermediates in the production of hollow ZrO_2 spheres. Theoretically, a 50 nm thick shell consisting of 5 nm ZrO_2 particles (packing density of 70%) on a nonporous 500 nm silica sphere would result in a specific surface area of about $120 \text{ m}^2 \text{ g}^{-1}$ (see ESI). Therefore, it seemed very unlikely that zirconia shells alone would result in materials with specific surface areas of more than $500 \text{ m}^2 \text{ g}^{-1}$. However, unambiguous conclusions were difficult to draw for the composite materials.

For this reason we have studied the generation of micropores within silica spheres obtained by a modified Stöber procedure that was adapted from the experiments leading to the above mentioned core-shell particles. The basic difference to the conventional Stöber process was a slightly different pre-treatment protocol of the silica particles, especially with respect to specific washing procedures. These modifications resulted in Stöber particles with surprisingly high micropore volumes. Here we report the details of

* Corresponding authors.

E-mail addresses: schmidt@kofo.mpg.de (W. Schmidt), schueth@kofo.mpg.de (F. Schüth).

¹ Current address: BASF Construction Solutions GmbH, D-83308 Trostberg, Germany.

² Current address: BASF SE, Carl-Bosch-Straße 38, D-67056 Ludwigshafen, Germany.

³ Current address: Centro de Tecnología de Recursos Minerales y Cerámica, Camino Centenario y 506, CC 49 (B1897ZCA), M.B. Gonnet, La Plata, Argentina.

that study and present experimental data that allow conclusions on the pore generation process.

2. Experimental section

2.1. Synthesis of monodisperse SiO_2 particles

Spherical silica particles were prepared following the well-known procedure described by Stöber and coworkers [1]. For the synthesis, 64 g of ethanol (LiChrosolv, Merck) and 22 g of an aqueous solution of NH_3 (Acros Organics, 28–30%) were mixed in a 500 mL glass flask. The flask was sealed with a septum and the solution heated under stirring to 30 °C. Then 4.2 mL of tetraethyl orthosilicate (TEOS) was rapidly injected into the solution. The system was left to react under stirring for 60 min over which a colloidal suspension of monodisperse siliceous particles formed. Then the solid phase was separated by centrifugation (5000 rpm, 5 min). After removal of the liquid, the solid was re-dispersed in 100 mL fresh de-ionized water. Solid separation and re-dispersion in water was repeated another two times (H_2O -00). Then, re-dispersion and centrifugation was repeated twice in 100 mL fresh alcohol. Finally, the obtained solid was re-dispersed in 100 mL of the respective alcohol for further processing (Et-01). In order to investigate the effect of the washing agent, a fraction of the samples was washed at that stage with de-ionized water instead of alcohol (H_2O -01). Next, the spherical silica particles dispersed in the alcohol were poured into a 500 mL single neck flask. The flask was sealed with a septum and heated under stirring to 30 °C. Subsequently, 0.5 mL of an aqueous solution of 0.43 g Lutensol AO5 (BASF), a non-ionic surfactant, in 11 g H_2O was added (Et-02), except for samples “noL” that were processed without addition of surfactant.

In the reaction route developed for the formation of core-shell materials [10], at this stage, one hour after addition of the surfactant, a metal alkoxide would have been added and the reaction would have been allowed to proceed overnight at 30 °C. In order to mimic that reaction in absence of the metal alkoxide, the reaction mixtures were kept at 30 °C overnight (Et-03 and noL-03). Subsequently, the liquid phase of the colloid was exchanged for water by centrifugation and re-dispersing the solid four times in

Table 1
Denotation of samples.

| Sample | Description | Step |
|--------------------------|--|-------|
| H_2O -00 | SiO_2 re-dispersed 3x in water | 00 |
| H_2O -01 | SiO_2 re-dispersed 6x in water | 01 |
| Et-xx | SiO_2 dispersed in ethanol | 01–05 |
| Et-xx-400 | Samples “Et” calcined at 400 °C | 01–05 |
| iPr-xx | SiO_2 dispersed in iso-propanol | 01–05 |
| Me-xx | SiO_2 dispersed in methanol | 01–05 |
| noL-xx | SiO_2 in ethanol without Lutensol AO5 | 01–05 |

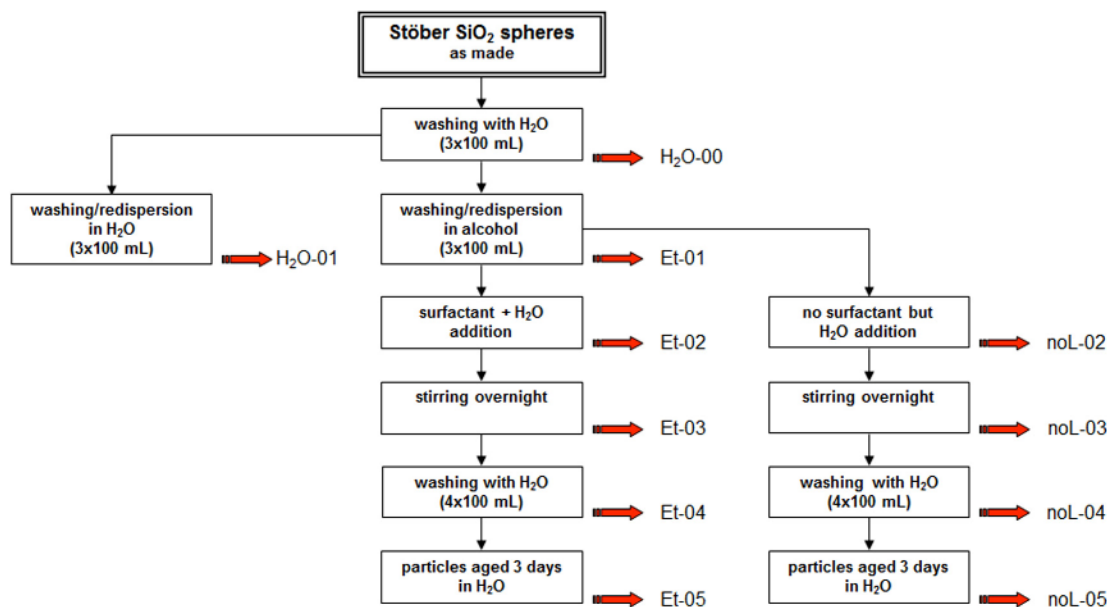
100 mL fresh de-ionized water (Et-04 and noL-04). Finally, the particles were aged in water at room temperature for three more days (Et-05 and noL-05). Scheme 1 summarizes a flow chart of the procedures.

Samples were collected with a syringe after each preparation step (0–5). The liquid aliquots were then centrifuged at 4500 rpm (Heraeus Multifuge 1L, Thermo Scientific) for 5 min. The liquid phases were decanted, until only about 1 mL of liquid was left which was then completely evaporated in air at 50 °C.

The sample codes for the samples are summarized in Table 1. “Et” stands for the SiO_2 dispersed in ethanol. The samples collected from subsequent process steps, as depicted in Scheme 1, are marked as –0x (steps 00–05). Thus, a sample collected after step 1, i.e., after dispersing the SiO_2 particles in ethanol, was denoted as Et-01 and so on. “iPr” stands for the SiO_2 dispersed in iso-propanol; “Me” for the SiO_2 dispersed in methanol; “noL” for the SiO_2 dispersed in ethanol, without addition of Lutensol AO5, “ H_2O -00” indicates particles collected after re-dispersing in water (three times 100 mL), “ H_2O -01” those re-dispersed three times in water (step 00) and then another three times in water (instead of alcohol; step 01).

2.2. Thermal treatment of SiO_2

After washing with water and drying, selected as-made Stöber particles were thermally treated under air by heating at a rate of 2 °C min⁻¹ to temperatures of 300 and 600 °C. Samples from the experiment with ethanol were calcined in air by heating at a rate of 2 °C min⁻¹ up to 400 °C and then cooled to room temperature (“Et-400”).



Scheme 1. Schematic overview of the synthesis pathways and denotation of the samples.

2.3. Characterization

Nitrogen sorption measurements at 77 K were performed on a Micromeritics ASAP 2010 sorption analyzer. Prior to the measurements, the samples were activated under vacuum for at least 7 h at 200 °C. Specific surface areas as well as apparent specific surface areas (for microporous samples for which the BET algorithm is strictly not appropriate) were calculated according to Brunauer-Emmett-Teller (BET) from the adsorption data in the relative pressure range of 0.02–0.15. Micropore volumes were calculated using the NLDFT kernel of the Autosorb software package provided by Quantachrome, applying a model of sorption of nitrogen in cylindrical pores in silica at 77 K on the adsorption branches of the isotherms. Porosities of the obtained silica spheres were estimated by Eq. (1).

$$\text{Porosity (\%)} = \frac{V_{\text{pore}} \times 100}{V_{\text{pore}} + 1/\rho}, \quad (1)$$

where V_{pore} is the total specific pore volume [$\text{cm}^3 \text{g}^{-1}$] determined using the adsorbed volume at a relative pressure of 0.995 from nitrogen sorption measurement and ρ the silica density that was assumed to be 2.2 g cm^{-3} [44].

High-resolution scanning transmission electron microscopy images were obtained with a Hitachi S-5500 high resolution scanning electron microscope with a cold field emission electron source operated at 2, 5 and 30 kV. All samples were prepared on a lacey carbon film supported on a copper grid.

^{13}C CP/MAS NMR spectra were measured on a Bruker Avance 500WB spectrometer using a 4-mm MAS probe at a spinning rate of 10 kHz. The spectra were recorded with a contact time of 1 ms, ^1H $\pi/2$ pulses of 5 μs and a repetition of 2 s (between 6000 and 24,000 scans). The chemical shift was referenced to neat TMS in a separate rotor.

IR spectra of powder samples were measured on a Nicolet Magna 560 FTIR spectrometer equipped with an ATR setup for measurements at ambient conditions.

Silicon contents of washing solutions were determined via photometric analysis at a commercial microanalytical laboratory (Mikroanalytisches Labor Kolbe, Mülheim an der Ruhr, Germany). In order to remove all residual solid silica particles from the solutions, the liquid fractions were isolated in an ultracentrifuge (Sigma, 3K30).

3. Results and discussion

Nitrogen adsorption isotherms of samples obtained using ethanol as the solvent are shown in Fig. 1. To avoid overloading of the figure with data points, only the adsorption branches of the isotherms are shown. The adsorption isotherms have been measured

on silica spheres that were obtained after individual preparation steps as outlined in Scheme 1. Reproduction of materials in independent syntheses showed that the applied synthesis protocol is quite robust. The average specific surface areas of materials that had been obtained in independent syntheses by different operators varied by about $\pm 6\%$. For consistency, only samples that were obtained successively from complete series will be discussed below.

Sample Et-01 that was obtained after washing the as-made Stöber particles with water and re-dispersing them in alcohol apparently consists of silica spheres with certain microporosity. However, the micropore volume of about $0.01 \text{ cm}^3 \text{g}^{-1}$ is rather low. Addition of aqueous surfactant solution (Et-02) and subsequent aging overnight (Et-03) both resulted in materials without any significant microporosity. Absence of micropores in these samples is also reflected by relatively low specific surface areas (see Table 2). Surprisingly, washing with water of these sample that had been aged in ethanol overnight finally resulted in silica spheres with very high apparent surface area of about $385 \text{ m}^2 \text{g}^{-1}$. This sample (Et-04) now also shows pronounced microporosity with a micropore volume of $0.13 \text{ cm}^3 \text{g}^{-1}$. In addition to the micropores, it also contains some smaller mesopores. The total pore volume of that sample is $0.2 \text{ cm}^3 \text{g}^{-1}$ and its estimated total porosity is about 31%. Keeping that sample in water for three more days slightly reduces the micropore volume and the apparent BET surface area but the total pore volume of that material (Et-05) remains basically unchanged.

For the desorption branches of some of the isotherms somewhat uncommon hysteresis shapes were observed. Pronounced hystereses are observed between adsorption and desorption branches. The hysteresis loops reproducibly did not close at a relative pressure of about 0.42 but remained unclosed down to relatively low desorption pressures (see Fig. S1 in ESI). This somewhat unusual desorption behavior could be due to the presence mesopores that are only accessible via micropores within the silica spheres. Presence of such a pore topology might result in trapping of adsorbed nitrogen in the mesopores down to low relative pressures. Another reason could be a rearrangement of the still flexible silica upon adsorption similar to the swelling effect that is often observed during gas adsorption in polymers. Cumulative pore size distributions of the different samples as calculated by the NLDFT method from the nitrogen adsorption branches of the isotherms are shown in Fig. 2 (see ESI for differential pore size distributions). Pores in the sample obtained directly after washing with water (Et-04) are mainly micropores ($<2 \text{ nm}$) with a smaller fraction of mesopores with sizes in the range of 2–4 nm. Keeping that sample in water for three more days (Et-05) resulted in a reduced micropore volume that is compensated by somewhat larger mesopores with sizes between 4 and 8 nm.

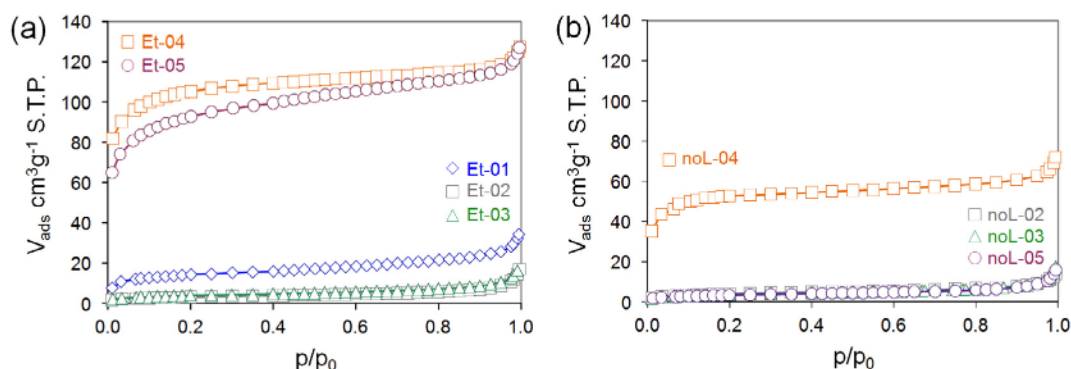


Fig. 1. Nitrogen adsorption isotherms of silica spheres that were obtained after individual preparation steps using ethanol as the solvent (a) with and (b) without using the surfactant Lutensol A05.

Table 2
Texture parameters for different Stöber particles.

| Sample | T_{\max} (°C) | S_{BET} ($\text{m}^2 \text{g}^{-1}$) | V_{mic} ($\text{cm}^3 \text{g}^{-1}$) | V_{pore} ($\text{cm}^3 \text{g}^{-1}$) | Porosity (vol%) |
|---------------------|------------------|---|--|---|-----------------|
| H ₂ O-00 | 200 ^a | 9 | 0.00 | 0.01 | 3 |
| H ₂ O-01 | 200 ^a | 14 | 0.00 | 0.02 | 3 |
| Et-01 | 200 ^a | 51 | 0.01 | 0.05 | 10 |
| Et-02 | 200 ^a | 12 | 0.00 | 0.03 | 6 |
| Et-03 | 200 ^a | 15 | 0.00 | 0.03 | 6 |
| Et-04 | 200 ^a | 385 | 0.13 | 0.20 | 31 |
| Et-05 | 200 ^a | 340 | 0.09 | 0.20 | 31 |
| noL-03 | 200 ^a | 12 | 0.00 | 0.01 | 2 |
| noL-04 | 200 ^a | 182 | 0.05 | 0.10 | 18 |
| noL-05 | 200 ^a | 12 | 0.00 | 0.02 | 3 |
| Me-01 | 200 ^a | 12 | 0.00 | 0.02 | 3 |
| Me-03 | 200 ^a | 7 | 0.00 | 0.01 | 3 |
| Me-04 | 200 ^a | 300 | 0.13 | 0.16 | 26 |
| Me-05 | 200 ^a | 402 | 0.16 | 0.20 | 31 |
| iPr-01 | 200 ^a | 64 | 0.01 | 0.04 | 8 |
| iPr-03 | 200 ^a | 6 | 0.00 | 0.01 | 2 |
| iPr-04 | 200 ^a | 14 | 0.00 | 0.02 | 4 |
| iPr-05 | 200 ^a | 350 | 0.12 | 0.18 | 28 |
| a.m. 300 | 300 ^c | 7 | – | 0.01 | 2 |
| a.m. 600 | 600 ^c | 8 | – | 0.01 | 2 |
| Et-01-400 | 400 ^c | 14 | 0.00 | 0.01 | 2 |
| Et-02-400 | 400 ^c | 13 | 0.00 | 0.01 | 2 |
| Et-03-400 | 400 ^c | 13 | 0.00 | 0.02 | 4 |
| Et-04-400 | 400 ^c | 253 | 0.09 | 0.14 | 24 |
| Et-05-400 | 400 ^c | 68 | 0.02 | 0.05 | 10 |

a.m.: as made Stöber particles calcined at different temperatures; T_{\max} : maximum temperature a given sample has been exposed to during (*) activation for sorption measurements or (°) calcination; S_{BET} : apparent surface area calculated by BET method; V_{mic} : micropore volumes calculated with NLDFT method; V_{pore} : total pore volume at $p/p_0 = 0.995$; Porosity: total porosity as calculated by Eq. (1); for sample denotations see Table 1.

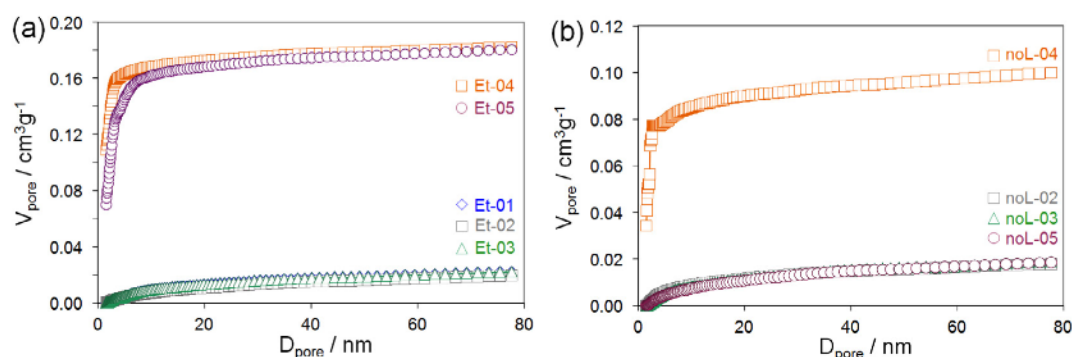


Fig. 2. Cumulative pore size distributions, as calculated with the NLDFT method, of silica spheres that were obtained using ethanol as the solvent after individual preparation steps (a) with and (b) without addition of Lutensol AO5.

Presence of micropores in Stöber particles has occasionally been observed by other groups as well [13,37,38,45]. However, to the best of our knowledge, micropore volumes that cause porosities of 30% have been never reported before. The micropore volumes observed here are almost comparable to those found in zeolites.

Performing the same synthesis but skipping the addition of the surfactant Lutensol AO5 results in somewhat different porosities of the particles. The highest pore volume was observed for sample noL-04. However, the total pore volume of sample noL-04 was only about half of that observed for sample Et-04. Similar as for sample Et-04, the majority of pores in sample noL-04 were micropores (Fig. 2). Keeping sample noL-04 in water for another three days resulted in a material with basically no remaining microporosity. The presence of Lutensol AO5 thus seems to be beneficial for the generation and stabilization of micropores.

For understanding the influence of ethanol on the micropore formation process, ¹³C CP/MAS NMR measurements were

performed. Fig. 3 shows the NMR spectra of samples that had been obtained with and without the addition of Lutensol AO5 as surfactant. For both reaction mixtures rather similar ¹³C CP/MAS NMR spectra are obtained. Spectra with resonance lines at 59 and 17 ppm that are typical of ethoxy groups (Et-O-Si) and ethanol are found in samples that were obtained after steps 01–03 [17,33]. Washing with water resulted in a complete removal of all ethanol and/or ethoxy species from the silica spheres. Already addition of water and stirring in that solution overnight (step 03) resulted in a significant reduction of ethoxy concentration within the particles. This reduction was more pronounced for the sample that had been obtained from the reaction mixture that contained the surfactant. Interestingly, no signals of the surfactant Lutensol AO5 are observed for the silica spheres which indicates that the surfactant is present mainly in the liquid phase. Lutensol AO5 thus seems to play a role in the dissolution and re-dispersion of material into the liquid phase.

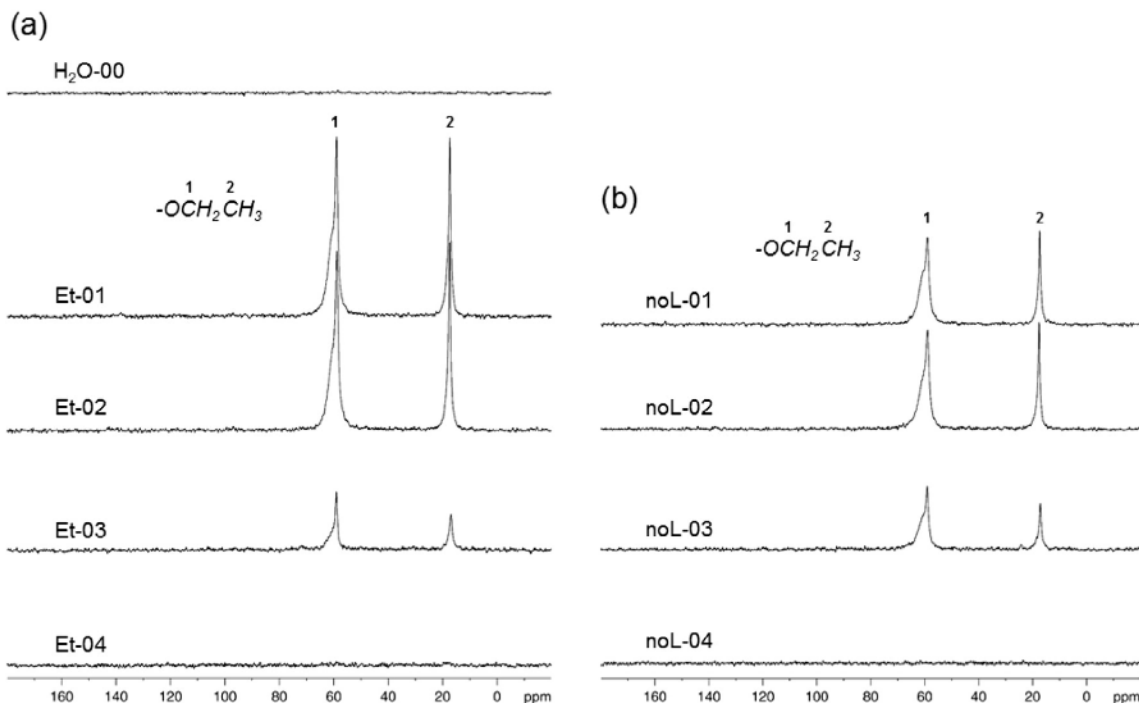


Fig. 3. ^{13}C CP/MAS NMR spectra of silica spheres that had been obtained using ethanol as the solvent after individual preparation steps (a) with and (b) without addition of Lutensol AOS (noL-01 corresponds to Et-01).

Surprisingly, the ^{13}C CP/MAS NMR spectrum of sample H₂O-00 that had been obtained by simply washing the as made Stöber particles three times with water does not show any indication of ethoxy species, i.e., sample H₂O-00 apparently does not contain any residual ethoxy groups or occluded ethanol. Since NMR is not very sensitive to small fractions of specific species, IR investigations on as made Stöber particles that had been treated with water were performed.

As can be seen in Fig. 4, bands due to ethanol and/or ethoxy species at 879, 1045, 1088, and in the ranges of 1270–1458 and 2888–2972 cm^{-1} are observed for as made Stöber particles. After washing these as-made particles only once with water, these bands have almost vanished and after washing the particles three times with water, the ethoxy signals cannot be detected any more.

Van Blaaderen et al. [17] among other authors [15,16,46], reported on the presence of several percent of ethoxy groups in

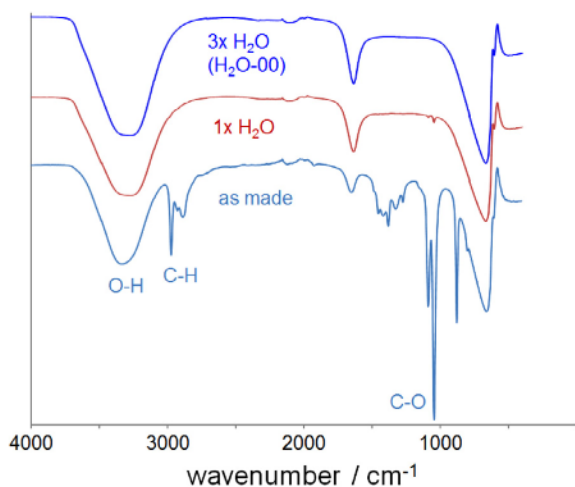


Fig. 4. FTIR spectra of as made Stöber silica particles and the same particles washed once and three times with water.

Stöber silica particles made from TEOS. The ethoxy groups are residues from the TEOS molecules that are not all fully hydrolyzed. However, according to the existing reports on silica particle formation from TEOS, the majority of the ethoxy groups is hydrolyzed to form ethanol, which is easily dialyzed and also lost by evaporation [47]. Residual ethoxy groups are believed to decrease the connectivity of the polysilicic acid chains, thus preventing the densification of the silica network and leaving also a greater proportion at a low degree of condensation, i.e., with a rather large amount of remaining silanol groups [48]. The existence of ethanol and/or ethoxy species in as made Stöber silica particles is confirmed by our results. However, simple exposure to water at room temperature results in quantitative hydrolysis of remaining alkoxide groups as shown here. In addition, the ethanol formed during the hydrolysis in water as well as ethanol that was formed within the silica particles during the Stöber process is completely extracted from the particles in water. This indicates that the amorphous silica framework is either still very flexible (swellable) or provides micropores that serve as diffusion pathways for exchange of ethanol by water. Furthermore, ethanol or ethoxy species that are present in the Stöber particles after re-dispersion in ethanol (Et-01, Et-02, Et-03) are inserted during exposure to the alcohol.

The Stöber particles that had been obtained after washing three times with water (H₂O-00) were basically nonporous. Also additional washing with water (H₂O-01) did not increase the porosity substantially (see Table 2 and isotherms in Fig. S2 in ESI). The Stöber silica particles that are obtained after simply washing them with water are thus almost non-porous, at least after drying for the sorption measurements. Why is it then that, after re-dispersion and storage in ethanol overnight (samples Et-03 and noL-03), washing with water results in the formation of micropores in the silica spheres?

The effect of washing with water has already been discussed in the literature [17,43]. It has been suggested that pore reconstruction may involve hydrolysis and condensation of silica [49], simultaneously with hydrolysis of alkoxide groups. As shown by our spectroscopic data, exposure of as made Stöber silica particles to

water results in complete hydrolysis of existing silicon ethoxide groups and extraction of ethanol from the silica spheres. In order to further understand the processes going on during the washing processes, it was very instructive to measure the concentrations of dissolved silica in the supernatant washing solutions as shown in Fig. 5. Even though the silica spheres possess no pronounced porosities after the first three washing steps with water, significant amounts of silica were released into the aqueous solutions (up to 0.47 mg mL^{-1} in one washing step) during these steps. Another fraction of the silica that is formed by the hydrolysis of alkoxide groups seems to remain as loosely condensed silica within the silica particles and blocks any existing pores. Such low-condensed silica species are very reactive. Therefore, re-dispersion in pure ethanol results in partial re-esterification of the highly abundant free silanol groups in the silica particles, may be accompanied by a certain swelling of the silica framework. Alcoholysis of Si–O–Si bonds probably also proceeds to form further alkoxide species. No dissolved silica was found in the alcoholic solutions (max. 0.003 mg mL^{-1}) as shown in Fig. 5. Thus only re-organization of the low-condensed silica within the particles takes place but no release of silicic species into the solutions. Particles that are formed during these process steps (Et-01, -02, -03) are still not very porous. However, they have somewhat higher porosities than the silica spheres after washing only with water (see Table 2). Finally washing the alcohol-treated silica particles again with water, results in hydrolysis of the newly formed alkoxide groups. The hydrolysis goes along with an additional release of silicic acid and oligomeric silica species into the aqueous solution, as shown in Fig. 5. Due to the additional removal of siliceous species after reorganization of the silica framework, now open pores are formed and the resulting particles have very high micropore volumes (Et-04, -05).

The reaction mixture for the Stöber synthesis contained 1.14 g silica (from 4.2 mL TEOS) which is basically consumed quantitatively for the generation of the silica spheres as can be seen from Fig. 5. The supernatant synthesis solution contained less than 0.0007 mg dissolved silica per 1 mL of solution. During the successive treatment with water, alcohol, and again water, a total of about 16 wt% of the parent silica was then redissolved. Assuming a typical density of precipitated silica of 2 g cm^{-3} , that amount of silica would correspond to a volume of about 0.08 cm^3 per gram. The volume of dissolved silica and the resulting micropore volumes are thus of comparable magnitude.

Assuming evenly distributed cylindrical pores throughout the complete spheres, geometrical calculations show that for such

micropore volumes the pore-to-pore distances within the silica spheres must be of the same magnitude as the pore diameters themselves (about 1.7–2 nm pore-to-pore distances for 2 nm pores, see ESI) as observed also for zeolites with channel-like pores. From these consideration it is very unlikely that the micropores are only located in a certain volume fraction of the silica spheres, e.g. close to the external surfaces. The pore walls would become too thin to maintain a stable silica particle. More likely the micropores extend throughout the entire silica spheres.

As shown above, the surfactant Lutensol AO5 does not act as a conventional porogen; it is not occluded in the particles as can be seen from NMR and FTIR spectra. It can only be active as surfactant on the surface of the Stöber particles or within the alcoholic solution. The surfactant most likely enhances the removal of loosely bound silica species from the particles, and thus larger micropore volumes are achieved if it is added to the silica particles. The drying of the Stöber spheres that are obtained at different steps of the above described process for sorption analyses may as well result in partial condensation of silanol groups, and reconstruction of the silica. The properties of the particles in solution therefore differ to a certain extent from those of the materials that are investigated in sorption experiments after activation at elevated temperature.

The data discussed above indicate that re-dispersion in ethanol and washing particles in water play important roles in the pore formation process. Especially the treatment in alcohol seems to be crucial since the rearrangement of the silica proceeds during that step. In order to investigate the effect of alternative alcohols on that process, we replaced ethanol against methanol or iso-propanol for re-dispersion.

Fig. 6 shows nitrogen sorption isotherms of silica particles which had been re-dispersed in methanol or iso-propanol, and then washed again with water. The isotherms show that microporous silica spheres can be generated also with these two alcohols. The numbers behind the alcohol denotation (Me- and iPr-) refer to the same process steps as used for the samples made with ethanol. Like particles that were obtained using ethanol for re-dispersion, silica spheres obtained with methanol or iso-propanol also possess high micropore volumes and high apparent specific surface areas. As shown in Table 2, the resulting silica spheres have micropore volumes of $0.16 \text{ cm}^3 \text{ g}^{-1}$ (Me-05) and $0.12 \text{ cm}^3 \text{ g}^{-1}$ (iPr-05) and apparent specific surface areas of about $400 \text{ m}^2 \text{ g}^{-1}$ (Me-05) and $350 \text{ m}^2 \text{ g}^{-1}$ (iPr-05).

The materials (-01 to -03) that were obtained after re-dispersion in either methanol or iso-propanol showed little porosity, in line with the results obtained with ethanol. The ^{13}C NMR spectra of these samples in Fig. 7 show that the processes taking place in

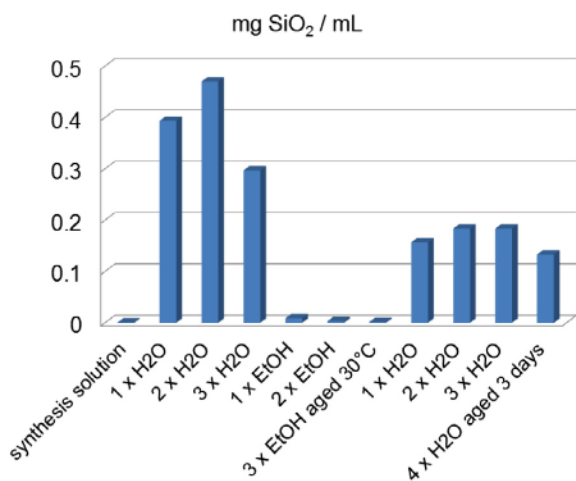


Fig. 5. Concentrations of dissolved silica in liquid phases after successive washing with water or ethanol.

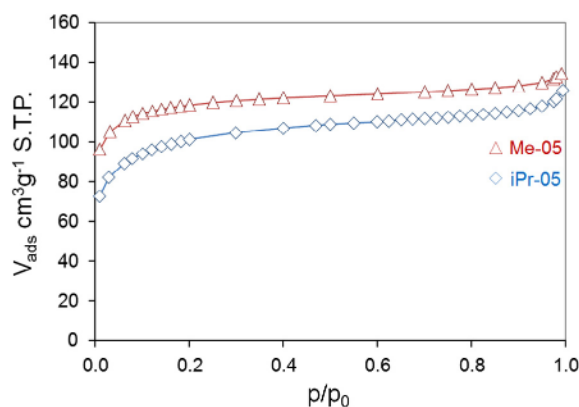


Fig. 6. Nitrogen adsorption isotherms of SiO₂ particles obtained from materials re-dispersed in methanol and iso-propanol.

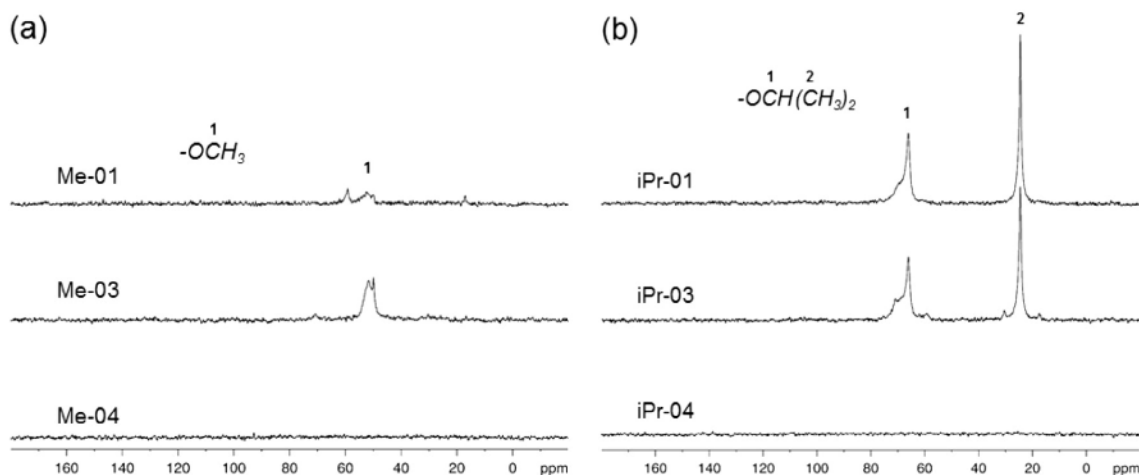


Fig. 7. ^{13}C CP/MAS NMR spectra of silica spheres re-dispersed in (a) methanol or (b) iso-propanol after washing of the as made particles with water.

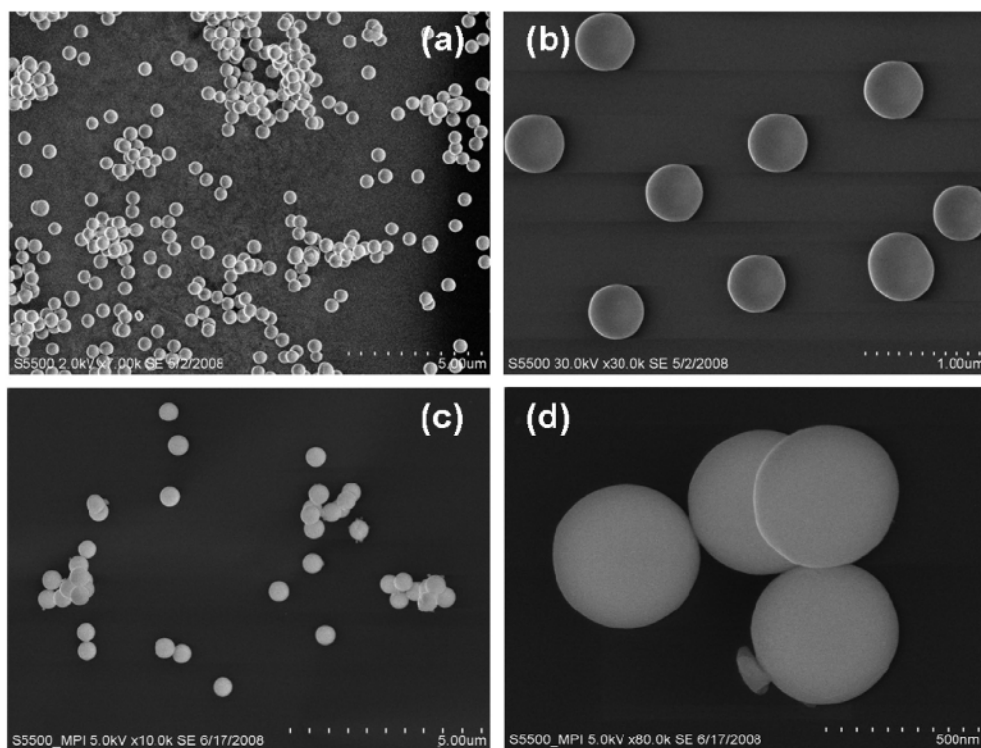


Fig. 8. SEM images of the silica spheres from the batch re-dispersed in ethanol Et-01 (a and b) and the particles washed with water Et-04 (c and d).

the silica particles upon immersion in the different alcohols are quite similar. As for ethanol, alkoxy groups are found for samples Me-01 to Me-03, and iPr-01 to iPr-03 after re-immersion of the silica spheres in the respective alcohols. As for the sample immersed in ethanol, no signals of the surfactant Lutensol AO5 are observed. After additional washing with water, no alkoxy species are present in the products Me-04, Me-05, iPr-04, and iPr-05. The processes taking place within the silica particles after re-immersion in alcohol thus seem to be very similar for the different alcohols. However, the micropore volumes of the final products vary slightly. For ethanol and methanol somewhat higher micropore volumes and total porosities are found than for iso-propanol.

The morphology of the spheres is more or less unaffected by the different types of post-synthesis treatment, as shown in Fig. 8. The SEM micrographs are representative for all investigated SiO_2 particles. The samples shown were collected after synthesis step 01 and 04, i.e., having substantially different porosities. All samples have a very narrow particle size distribution, and all particles are almost perfect spheres with a mean diameter of about 490 nm. From the images shown, the diameter of the native particles might be somewhat underestimated, since under electron irradiation the Stöber spheres may shrink by up to 5% [11,17,37].

Finally, the effect of thermal treatment on the porosities of different Stöber particles was investigated. Calcination of as made

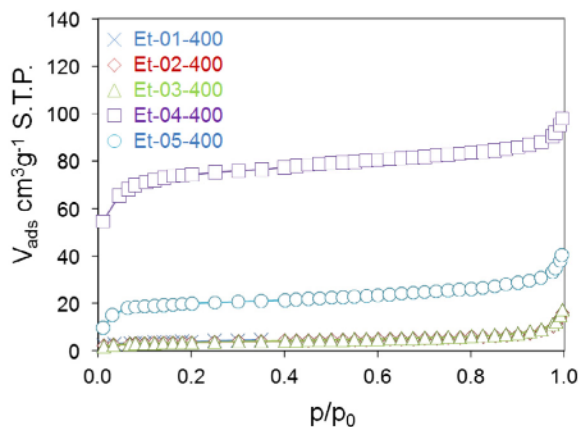


Fig. 9. Nitrogen adsorption isotherms of SiO₂ particles after calcination at 400 °C.

Stöber silica spheres at different temperatures between 300 and 600 °C did not result in particles with substantial porosity. As listed in Table 2, samples a.m.300 and a.m.600 show very low surface areas of only about 7–8 m² g⁻¹ and basically no microporosity. Also samples that were calcined at 400 °C after re-immersion in ethanol show hardly any microporosity and specific surface areas of less than 10 m² g⁻¹. However, calcination of particles obtained after synthesis steps 04 and 05 at 400 °C preserved a substantial fraction of micropores, as shown in Fig. 9. Calcination generally resulted in a decrease of micropore volumes, most likely caused by shrinkage of the larger pores and structure densification. Nevertheless, a substantial number of micropores persist during calcination, especially for particles that have been obtained after step 4.

The results of this study may have wide ranging implications. Firstly, they help explaining some of the controversial statements that can be found in literature concerning porosity of Stöber-type silica particles. Slight differences in synthetic protocols, especially following the generation of the particles itself, can be responsible for observed differences. Secondly, Stöber silica materials are important in a number of different applications, such as chromatography or the generation of colloidal crystals. For such applications it is obviously important to control the porosity. The possibility to introduce porosity in a controlled manner opens up doors to novel applications, e.g., in separation and/or chromatography. Finally, the microporosity is crucial for some applications where Stöber particles are used as sacrificial templates for the generation of rattle-type particles. The embedded core particles are accessible via the micropores and can be functionalized to some extent within the silica shell. This can be advantageous in tailoring the properties of such composite systems, as has been shown in the controlled size adjustment of gold particles embedded in such microporous Stöber silica [38].

4. Conclusions

In conclusion, Stöber silica spheres with surprisingly high micropore volumes up to about 0.16 cm³ g⁻¹ are formed during post-synthesis treatment with alcohol and water. The development of the micropores is caused by repetitive hydrolysis and re-esterification of residual alkoxide groups in the as-made silica, accompanied by successive silica reorganization and condensation. Different alcohols can be used for re-esterification of the particles upon re-immersion of the silica in the alcohols. However, the total pore volumes that are generated with the different alcohols differ slightly. The surfactant Lutensol AO5 enhances the micropore formation, but is not essential for that process. Micropores are generated in Stöber silica particles by a series of simple consecutive

steps, i.e., thorough washing of as made Stöber silica particles with water, re-immersing them in alcohol for a couple of hours and washing them again with water.

Acknowledgements

The financial support from the Deutsche Forschungsgemeinschaft (SFB 558), in addition of the basic funding by the Max Planck Gesellschaft, is gratefully acknowledged. We would like to thank Caroline Gawlik for support in preparative work and Hans-Josef Bongard for electron microscopic analysis.

Appendix A. Supplementary data

Supplementary data associated with this article can be found, in the online version, at <http://dx.doi.org/10.1016/j.micromeso.2014.07.051>.

References

- [1] W. Stöber, A. Fink, E. Bohn, *J. Colloid Interface Sci.* 26 (1968) 62–69.
- [2] R.K. Iler, *The Chemistry of Silica*, John Wiley & Sons, New York, 1979, pp. 528–599.
- [3] J. Wang, H. Leeman, R.A. Schoonheydt, *Catal. Today* 112 (2006) 188–191.
- [4] E. Mathiowitz, J.S. Jacob, Y.S. Jong, G.P. Carino, D.E. Chickering, P. Chaturvedi, C.A. Santos, K. Vijayaraghavan, S. Montgomery, M. Bassett, C. Morrell, *Nature* 386 (1997) 410–414.
- [5] C. Boissière, M. Kümmler, M. Persin, A. Larbot, E. Prouzet, *Adv. Funct. Mater.* 11 (2001) 129–135.
- [6] A. Kurganov, K.K. Unger, T. Issaeva, *J. Chromatogr. A* 753 (1996) 177–190.
- [7] U. Trüding, G. Müller, K.K. Unger, *J. Chromatogr. A* 535 (1990) 111–125.
- [8] A. Blanco, E. Chomski, S. Gräbtl, M. Ibisate, S. John, S.W. Leonard, C. Lopez, F. Meseguer, H. Miguez, J.P. Mondia, G.A. Ozin, O. Toader, H.M. van Driel, *Nature* 405 (2000) 437–440.
- [9] H.A. Ketelson, R. Pelton, *M.A. Brook, Langmuir* 12 (1996) 1134–1140.
- [10] P.M. Arnal, C. Weidenthaler, F. Schüth, *Chem. Mater.* 18 (2006) 2733–2739.
- [11] A. van Blaaderen, J. Van Geest, A.J. Vrij, *J. Colloid Interface Sci.* 154 (1992) 481–501.
- [12] G.H. Bogush, C.F. Zukoski IV, *J. Colloid Interface Sci.* 142 (1991) 1–18.
- [13] H. Giesche, *J. Eur. Ceram. Soc.* 14 (1994) 189–204.
- [14] A.J. Lecloux, J. Bronckart, F. Noville, C. Dodet, P. Marchot, J.P. Pirard, *Colloids Surf.* 19 (1986) 359–374.
- [15] T. Matsoukas, E. Gulari, *J. Colloid Interface Sci.* 124 (1988) 252–261.
- [16] T. Matsoukas, E. Gulari, *J. Colloid Interface Sci.* 132 (1989) 13–21.
- [17] A. van Blaaderen, A.P.M. Kentgens, *J. Non-Cryst. Solids* 149 (1992) 161–178.
- [18] A. Burneau, B. Humbert, *Colloids Surf. A* 75 (1993) 111–121.
- [19] J. Look, G.H. Bogush, C.F. Zukoski, *Faraday Discuss. Chem. Soc.* 90 (1990) 345–357.
- [20] L. Jelinek, P. Dong, C. Rojas-Pazos, H. Taïbi, E. Kováts, *Langmuir* 8 (1992) 2152–2164.
- [21] A.P. Philipse, *Colloid Polym. Sci.* 266 (1988) 1174–1180.
- [22] G.H. Bogush, M.A. Tracy, C.F. Zukoski IV, *J. Non-Cryst. Solids* 104 (1988) 95–106.
- [23] A. Vrij, J.W. Jensen, J.K.G. Dhont, C. Pathmamanoharan, M.M. Kops-Werkhoven, H.M. Fijnaut, *Faraday Discuss. Chem. Soc.* 76 (1983) 19–35.
- [24] S. Masse, G. Laurent, F. Chuburu, C. Cadiou, I. Déchamps, T. Coradin, *Langmuir* 24 (2008) 4026–4031.
- [25] H.A. Ketelson, M.A. Brook, R.H. Pelton, *Polym. Adv. Technol.* 6 (1995) 335–344.
- [26] P. Auroy, L. Auvray, L. Léger, *J. Colloid Interface Sci.* 150 (1992) 187–194.
- [27] C. Pathmamanoharan, *Colloids Surf.* 50 (1990) 1–6.
- [28] J. Clarke, B. Vincent, *J. Colloid Interface Sci.* 82 (1981) 208–216.
- [29] M. Grün, G. Büchel, D. Kumar, K. Schumacher, B. Bidlingmajer, K.K. Unger, *Stud. Surf. Sci. Catal.* 128 (2000) 155–165.
- [30] M. Grün, I. Lauer, K.K. Unger, *Adv. Mater.* 9 (1997) 254–257.
- [31] Q. Luo, L. Li, Z. Xue, D. Zhao, *Stud. Surf. Sci. Catal.* 129 (2000) 37–41.
- [32] H.A. Ketelson, M.A. Brook, R. Pelton, *Chem. Mater.* 7 (1995) 1376–1383.
- [33] A. van Blaaderen, A. Vrij, *J. Colloid Interface Sci.* 156 (1993) 1–18.
- [34] R.D. Badley, W.T. Ford, F.J. McEnroe, R.A. Assink, *Langmuir* 6 (1990) 792–801.
- [35] J.W. Goodwin, R.S. Harbron, P.A. Reynolds, *Colloid Polym. Sci.* 268 (1990) 766–777.
- [36] A.P. Philipse, A. Vrij, *J. Colloid Interface Sci.* 128 (1989) 121–136.
- [37] A.K. van Helden, J.W. Jansen, A. Vrij, *J. Colloid Interface Sci.* 81 (1981) 354–368.
- [38] R. Güttel, M. Paul, F. Schüth, *Chem. Commun.* 46 (2010) 895–897.
- [39] A. Labrosse, A. Bumeau, *J. Non-Cryst. Solids* 221 (1997) 107–124.
- [40] D.L. Green, S. Jayasundara, Y.-F. Lam, M.T. Harris, *J. Non-Cryst. Solids* 315 (2003) 166–179.
- [41] R. Güttel, M. Paul, F. Schüth, *Catal. Sci. Technol.* 1 (2011) 65–68.
- [42] C. Galeano, R. Güttel, P. Michael, P. Amal, A.H. Lu, F. Schüth, *Chem. Eur. J.* 17 (2011) 8434–8439.
- [43] P.M. Arnal, M. Comotti, F. Schüth, *Angew. Chem. Int. Ed.* 45 (2006) 8224–8227.

- [44] T. Dabadie, A. Ayrat, C. Guizard, L. Cot, P. Lacau, *J. Mater. Chem.* 6 (1996) 1789–1794.
- [45] A. Walcarius, C. Despas, J. Bessière, *Micropor. Mesopor. Mater.* 23 (1998) 309–313.
- [46] M.T. Harris, R.R. Brunson, C.H. Byers, *J. Non-Cryst. Solids* 121 (1990) 397–403.
- [47] G. Büchel, K.K. Unger, A. Matsumoto, K. Tsutsumi, *Adv. Mater.* 10 (1998) 1037–1038.
- [48] C.A.R. Costa, C.A.P. Leite, F. Galembeck, *J. Phys. Chem. B* 107 (2003) 4747–4755.
- [49] P.J. Davis, R. Deshpande, D.M. Smith, C.J. Brinker, R.A. Assink, *J. Non-Cryst. Solids* 167 (1994) 295–306.